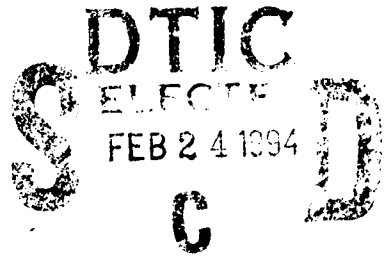


# FINAL REPORT

for

15 September, 1990 through 14 September, 1993

for

## Office of Naval Research

Grant No. N00014-90-J-4071

# Numerically Stable Algorithms in String Dynamics

Alan J. Laub and Charles Kenney, Principal Investigators

Department of Electrical & Computer Engineering
University of California
Santa Barbara, CA 93106-9560

ph.: (805) 893-3616
fax: (805) 893-3262
e-mail: laub@ece.ucsb.edu

## I. Factual Data

This section contains a factual listing of publications, research lectures, and personnel supported in whole or in part under ONR Grant No. N00014-90-J-4071. The narrative to follow in Section II will be keyed to the item numbers in these lists. Copies of the abstracts of published and submitted papers will follow in Section III.

### A. Papers Published in Refereed Journals

1. Overfelt, P.L. and C.S. Kenney, "Comparison of the Propagation Characteristics of Bessel, Bessel-Gauss, and Gaussian Beams Diffracted by a Circular Aperture," *J. Optical Soc. of America A*, Vol. 8, No. 5, May 1991.
2. Kenney, C.S. and P.L. Overfelt, "A Simple Approach to Mode Analysis for Parabolic Waveguides," *IEEE Trans. Microwave Th. and Tech.*, Vol. 39, No. 3, March 1991.
3. Hench, J.J., C.S. Kenney, and A.J. Laub, "Methods for the Numerical Integration of Hamiltonian Systems," to appear in *Circuits, Systems, and Signal Processing*, 1994.

### B. Papers Submitted to Refereed Journals

None.

### C. Books (and sections thereof) Published

1. Kenney, C.S. and P.L. Overfelt, "Optimizing Waveguide Cross-Sections with Respect to Power Handling Capability," *Trends in Microwave Theory and Techniques 1*, to appear.



### D. Papers Published in Refereed Conferences

None.

### E. Invited Presentations Including Scientific/Technical Society Conferences

None.

## F. Contributed Presentations at Scientific/Technical Society Conferences

1. *Helical Solutions to Fiber-Payout Problems*: for the Fifth Tri-Service Conference on Fiber Optic Guided Missiles, Naval Ocean Systems Center, San Diego, CA, November 5-7, 1990.
2. *Inner and Outer Modes for Fiber Dynamics*: for the Sixth Tri-Service Conference on Fiber Optic Guided Missiles, Naval Postgraduate School, Monterey, CA, March 18-21, 1991.

## G. Technical Reports Published or Non-refereed Journals

1. Hench, J.J., C.S. Kenney, and A.J. Laub, "A Padé-Magnus Method for the State Transition Calculation of a Linear Time-Varying System," Technical Report SCL 91-03, University of California, Santa Barbara, Electrical and Computer Engineering Dept., September, 1991.
2. Kenney, C.S., "Inner and Outer Wave Modes For Fiber Dynamics," Naval Weapons Center Technical Paper No. NWC TP 7149, June 1991.

## H. Patents

1. Hoban, F., G. Hewer, D. Harms, and C. Kenney, patent applied for "Internal Fiber Optics Payout System with Rotary Drive and Control," Navy Case No. 73679, June 5, 1991.
2. Hoban, F., G. Hewer, D. Harms, and C. Kenney, patent applied for "Rotary Controlled Payout Device," Navy Case No. 71410, Oct. 21, 1991.

## I. Researchers Supported in Whole or in Part by the Grant

RESEARCH ENGINEER

Charles Kenney (half-time support)

# II. Narrative

In this section, we provide a summary of the research conducted during the period September 1990 to September 1993. Because of an administrative oversight, funding for this grant covered only the period September 1990 through September 1991. All research conducted subsequent to September 1991 was unfunded. A more detailed description of some of our research topics is contained in the original proposal for the grant.

The main goal of our work was to develop sound numerical algorithms for solving the partial differential equations that arise in string dynamics problems, especially of the type encountered by fiber optic guided missiles. In pursuit of this goal, we worked closely with engineers (Fay Hoban and others) and mathematicians (Gary Hewer) and physicists (Pam Overfelt) involved in the SKYRAY project at the Naval Weapons Center in China Lake, California. SKYRAY was a demonstration project for fiber payout at high velocities (800 ft/sec and greater) and this cooperative effort resulted in two patent applications: a novel inside payout design and a rotating outer payout design (see H.1 and H.2 respectively above and the discussion below).

The partial differential equations that describe fiber payout (see the grant proposal) reduce to ordinary differential equations subject to boundary conditions in the case of uniform rotary motion. This reduction served as the point of departure for our study for several reasons. First, the assumption of uniform rotary motion is very close to that measured experimentally, and at the same time reduces the number of system parameters to a small group that can be easily varied for design studies. Secondly, the resulting ODE BVP can be solved exactly in terms of elliptic sine functions for the special case of inner payout with zero air resistance (see G.2 above). This is significant because the inner payout modes are very insensitive to changes in air resistance, and consequently can be well modeled by the zero resistance case. Moreover, the inner payout boundary conditions can be used (in a half wave number mode) to generate approximate boundary conditions for the outer payout modes. The vector form of Newton's method then provides a way of finding the true boundary conditions for the outer modes. The details describing this procedure were developed in a series of eight unpublished working notes for the design group at NWC and summarized in G.2. Subsequently we implemented these procedures as MATLAB macros in a software package called FIBERPACK. During the testing of this package we discovered that the inner payout modes produced far less tension in the fiber compared to the outer modes especially during high-altitude simulations. We also found that rotating the bobbin to assist payout reduces the tension even further. Reductions of this kind are crucial to high-speed payout because the tension increases as the square of the payout velocity. These observations formed the basis of the rotating and inner payout design patent applications mentioned above.

Problems related to signal attenuation during fiber transmission were also considered. Working with Pam Overfelt of the Physics Division at NWC, we developed a variety of methods for analyzing and optimizing power-handling characteristics as well as modes of propagation (see A.1, A.2, and C.1). The principal benefit of these studies has been an increased awareness of the signal attenuation caused by sharp kinks or bends in the fiber. Such kinks appear to be exaggerated by torsion effects related to payout designs which use constraining shrouds as described below.

In future research it would be desirable to extend our effort to include problems in which the fiber contacts a constraining shroud and may suffer time-varying impluse forces. The shroud problem is of interest because of the need to force the fiber in certain directions, such as away from the rocket plume. The shroud-fiber contact point induces a torsion effect into the governing differential equations that makes numerical computation difficult and is sure to produce some interesting results.

Time-varying impulse forces also need to be studied because the payout environment is subject to extreme aerodynamic forces and because the design engineers at NWC want to use high frequency dither to reduce frictional effects at the shroud contact point. The simplest models of these forces result in ordinary differential equations with time-varying coefficients. Fortunately we were able to complete an initial study of this problem in A.3 and it appears that very efficient solution procedures are possible.

We are excited about the progress that was made, but many important open research problems remain.

## III. Abstracts of Published and Submitted Papers

See attached.

# Comparison of the propagation characteristics of Bessel, Bessel–Gauss, and Gaussian beams diffracted by a circular aperture

P. L. Overfelt and C. S. Kenney

*Physics Division and Applied Mathematics Group, Research Department, Naval Weapons Center, China Lake, California 93555-6001*

Received June 14, 1990; accepted December 19, 1990

We use the scalar Kirchhoff–Huygens diffraction integral to obtain analytic expressions for both axial and transverse intensity distributions, assuming normal incidence on a circular aperture for four types of incident field: (1) plane wave, (2) Bessel beam, (3) Gaussian beam, and (4) Bessel–Gauss beam. We use the Fresnel approximation to obtain the axial intensity as a function of distance from the aperture. We consider both Fresnel and Fraunhofer diffraction for the case of the transverse intensity distributions. For the axial case, we find that the Bessel–Gauss beam performs worse than the Bessel beam, in terms both of the magnitude of intensity and of its ability to extend a distance from the aperture. In the transverse case, we find that the Bessel–Gauss beam performance in terms of remaining nearly diffraction free over a given distance is highly dependent on the relationship among the aperture radius, the beam waist parameter, and the transverse wave number.

## 1. INTRODUCTION

Recently, there has been much interest in the possible propagation of diffraction-free beams at optical frequencies.[1–3] These include the Bessel beam[1,2] and the Bessel-Gauss beam.[3] In previous work the Bessel-Gauss beam has been considered only for free-space propagation, while the Bessel beam was analyzed by numerical simulation and verified subsequently through experiment.

In what follows we use scalar Kirchhoff theory to obtain analytic expressions for the axial and transverse intensity distributions, assuming normal incidence upon a circular aperture for four types of field: (1) plane wave, (2) Bessel beam, (3) Gaussian beam, and (4) Bessel–Gauss beam. Since the Bessel–Gauss beam is the most general of the incident fields considered above, once its intensity distribution is found the distributions of the remaining fields can be recovered by using limiting cases of the Bessel–Gauss intensity function. The analysis for the axial intensity is shown in Section 2, and that for the transverse intensity is shown in Section 3. In Section 4 we discuss the Fraunhofer diffraction pattern generated by an incident Bessel beam and show that the amount of energy contained within any specified radius can be controlled by changing the value of the transverse wave number, which governs the sharpness of the central maximum of the Bessel beam. Section 5 contains our conclusions.

## 2. AXIAL INTENSITY IN THE FRESNEL REGION

Assuming $\exp(i\omega t)$ time dependence throughout, cylindrical coordinates $(\rho, \phi, z)$ and incident fields that are cylindrically symmetric (independent of $\phi$), the scalar Kirchhoff–Huygens diffraction integral (for normal incidence) is given by[4]

$$\psi(\rho, z) = \frac{ik_0}{2\pi} \int_A \psi_{\mathrm{inc}}(\rho', 0) \frac{\exp(-ik_0 R)}{R}\, dA, \tag{1}$$

where $A$ is the aperture in a plane screen, $k_0 = 2\pi/\lambda_0$ is the free-space wave number, $\psi_{\mathrm{inc}}(\rho', 0)$ is the incident field at $z' = 0$, and

$$R = [\rho'^2 + \rho^2 + z^2 - 2\rho\rho' \cos(\phi' - \phi)]^{1/2}. \tag{2}$$

For the case of axial intensity as a function of distance from the aperture in the upper half-plane, $z > 0$ (see Fig. 1), we set $\rho = 0$. Thus Eq. (2) becomes

$$R = (\rho'^2 + z^2)^{1/2}, \tag{3}$$

$$R = z\left[1 + \frac{1}{2}\left(\frac{\rho'}{z}\right)^2 - \frac{1}{8}\left(\frac{\rho'}{z}\right)^4 + \ldots\right], \tag{4}$$

$$R \approx z + \frac{\rho'^2}{2z}, \tag{5}$$

by using the Fresnel approximation for $R$; i.e., $R \approx z$ in the denominator and $R$ given by relation (5) in the exponential portion of Eq. (1). The scalar diffracted field given by Eq. (1) becomes

$$\psi(0, z) = \frac{ik_0}{2\pi} \frac{\exp(-ik_0 z)}{z} \times \int_0^{2\pi} \int_0^a \psi_{\mathrm{inc}}(\rho', 0) \exp(-ik_0 \rho'^2/2z) \rho' d\rho' d\phi' \tag{6}$$

for a circular aperture of radius $a$ in a plane screen. At this point, we should note that the Raleigh–Sommerfeld integral (in the paraxial limit) would have led to Eq. (6) also (as was pointed out by an unknown reviewer). We want to evaluate Eq. (6) for four incident fields: plane wave, Bessel beam,

IEEE TRANSACTIONS ON MICROWAVE THEORY AND TECHNIQUES, VOL. 39, NO. 3, MARCH 1991



# A Simple Approach to Mode Analysis for Parabolic Waveguides

Charles S. Kenney, *Associate Member, IEEE*, and P. L. Overfelt, *Member, IEEE*

*Abstract*—**Difficulty in obtaining accurate values for parabolic cylinder functions has been an impediment to mode analysis for parabolic waveguides. A simple method, based on one-dimensional analytic continuation, is presented which gives essentially exact values for these functions; i.e., the relative error in the computed result is on the order of the machine round-off. When supplemented with a Newton–Poisson shooting method and simple homotopy techniques, this continuation method can be used to find the TE and TM mode eigenvalues, and associated separation constants, for arbitrary parabolic domains. These methods are then used to compute a power handling efficiency factor for a range of parabolic regions.**

## I. Introduction

We consider parabolic cylinders of uniform cross section in the confocal parabolic coordinates $(\xi, \eta, z)$, which are related to rectangular coordinates $(X, Y, Z)$ via

$$X = \frac{1}{2}(\eta^2 - \xi^2) \qquad Y = \eta\xi \qquad z = Z \quad (1)$$

(see Fig. 1). The cross sections of interest consist of the interior regions $\Omega = \Omega(\xi_0, \eta_0)$ bounded on the right by the curve $\eta = \eta_0$ and on the left by the curve $\xi = \xi_0$.

Assuming a uniform, perfectly conducting waveguide of parabolic cross section with $e^{-i\beta z}e^{i\omega t}$ dependence, we use

$$\psi = \begin{Bmatrix} E_z \\ H_z \end{Bmatrix}$$

where $\psi$ satisfies

$$\psi_{XX} + \psi_{YY} = -k^2\psi \qquad \text{in } \Omega \qquad (2)$$

subject to the boundary conditions,

$$E_z = 0 \qquad \text{on } \partial\Omega \text{ (TM modes)} \qquad (3)$$

or

$$\frac{\partial H_z}{\partial n} = 0 \qquad \text{on } \partial\Omega \text{ (TE modes)}. \qquad (4)$$

Here $\partial\Omega$ denotes the boundary of $\Omega$, $\partial/\partial n$ is the outward normal derivative, and variable subscripts indicate differentiation. In (2), $k^2 = k_0^2 - \beta^2$ and $k_0^2 = \omega^2\epsilon_0\mu_0$.

Manuscript received January 23, 1990; revised November 19, 1990. This work was supported in part by the National Science Foundation under Grant DMS88-00817 and by the Air Force Office of Scientific Research under Contract AFOSR-89-0167.

C. S. Kenney is with the Electrical and Computer Engineering Department, University of California, Santa Barbara, CA 93106, and the Naval Weapons Center, China Lake, CA 93555.

P. L. Overfelt is with the Physics Division, Research Department, Naval Weapons Center, China Lake, CA 93555-6001.

IEEE Log Number 9042353.

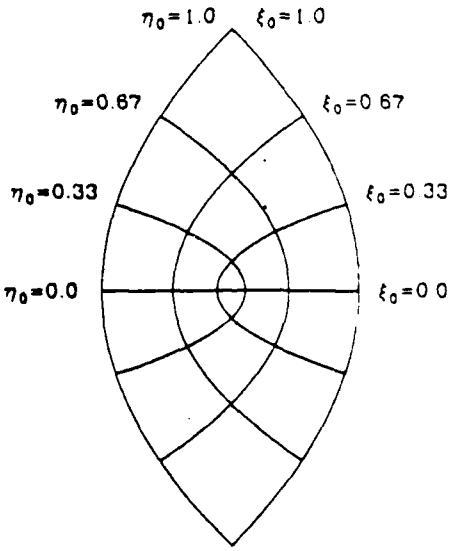


Fig. 1. Confocal parabolic regions.

Expressing (2) in parabolic coordinates gives

$$\psi_{\xi\xi} + \psi_{\eta\eta} = -k^2(\xi^2 + \eta^2)\psi. \qquad (5)$$

Using separation of variables with $\psi = U(\xi)V(\eta)$ we find

$$U_{\xi\xi} + (k^2\xi^2 + \alpha)U = 0 \qquad (6)$$

$$V_{\eta\eta} + (k^2\eta^2 - \alpha)V = 0 \qquad (7)$$

where $\alpha$ is the separation constant. Equations (6) and (7) must be supplemented by the boundary conditions

$$U(\xi_0) = 0 \qquad V(\eta_0) = 0 \qquad \text{(TM modes)} \qquad (8)$$

or

$$U_\xi(\xi_0) = 0, \qquad V_\eta(\eta_0) = 0 \qquad \text{(TE modes)}. \qquad (9)$$

Although (6) and (7) can be solved for any $\alpha$ and $k$, the boundary conditions (8) and (9) are satisfied only at discrete pairs $(\alpha, k)$, when $\xi_0$ and $\eta_0$ are fixed.

In the following section, we show that solutions to (6) and (7) can be computed via one-dimensional analytic continuation. Section III discusses a Newton–Poisson shooting method for finding the separation constants, $\alpha$, and eigenvalues, $k$, for fixed $\xi_0$ and $\eta_0$. This method is easy to use and reveals some inaccuracies in previously published work. In particular, Tables I and II give pairs of values $(a, q) = (\alpha/2k, \sqrt{2k})$ to seven significant digits for the case $\xi_0 = \eta_0$, and show that some entries in similar tables from [1] have only one digit of accuracy. The values in Tables I and II were used to generate (via a simple homotopy method) the eigen-

# Methods for the Numerical Integration of Hamiltonian Systems*

J.J. Hench, C.S. Kenney, and A.J. Laub
Department of Electrical and Computer Engineering
University of California
Santa Barbara, CA 93106-9560

**Abstract**

In order to compute an infinite horizon optimal controller for a linear periodic system via an invariant subspace method, the computation of the period map associated with the Hamilton-Jacobi-Bellman equations is required. In this paper we discuss methods for the numerical integration of such Hamiltonian systems. Two numerical integration techniques are introduced. A method is developed whereby symplectic invariants associated with the Hamilton-Jacobi-Bellman equations are preserved. Also, a shifting scheme is introduced which in effect swaps the roles of the stable and unstable invariant subspaces by using the semigroup property of state transition matrices. A shift is introduced into the resultant initial value problem assuring that the eigenvalues of a differential equation reside in the region of absolute stability for an appropriate numerical integration routine. These techniques are then compared to standard numerical integration routines to ascertain their efficiency and accuracy.

*Keywords*: Padé approximation, linear systems, periodic systems, periodic Riccati equation, state transition matrix, invariant subspaces.
*AMS(MOS) subject classification*: 65L05
*Abbreviated title*: Numerical Integration of Hamiltonian Systems.

## 1 Introduction

In this paper, we examine various methods of computing the optimal feedback controller gains for linear, periodic time-varying systems

$$\dot{x}(t) = A(t)x(t) + B(t)u(t) \tag{1}$$

with quadratic cost functional:

$$\min_u \frac{1}{2}\int_0^\infty \left[x^T Q(t)x + u^T R(t)u\right] dt \tag{2}$$

*This research was supported by the Air Force Office of Scientific Research under Grant No. AFOSR-91-0240, the National Science Foundation under Grant No. ECS-9120643, and the Office of Naval Research under Grant No. N00014-90-J-4071 and No. N00014-92-J-1706.

Trends in Microwave Theory & Techniques, 1

# Optimizing waveguide cross- sections with respect to power handling capability

**C.S. Kenney[1], P.L. Overfelt[2]**

1. Department of Electrical and Computer Engineering, University of California, Santa Barbara, CA-93106 2. Physics Division, Research Department, Naval Weapons Centre, China Lake, CA-93555-6001, USA.

## ABSTRACT

An analysis is given of the power-handling capabilities of four families of waveguide cross-sectional shapes, including rectangular, elliptical, parabolic and rhombic. Using an efficiency factor based on the two lowest TE modes, it is seen that ellipses are slightly better than the standard 2:1 rectangular waveguide and that for the waveguides considered here, power- handling is maximized when the second and third TE mode eigenvalues are equal. Since this efficiency factor is relatively insensitive to slight variations in cross-sectional shape, good estimates of power-handling capability can be made by comparison with rectangular shapes or other simple geometries of the same aspect ratio.

## INTRODUCTION

This paper addresses the problem of finding the waveguide cross-sectional shape, $\Omega$, which optimises power handling capability as measured by the efficiency factor, $\gamma$, defined by Baum (1988). This general problem is difficult because $\gamma$ depends on the first two TE modes of $\Omega$, i.e. the first two eigenvalues of the Laplacian over $\Omega$ with Neumann boundary conditions:

$$\Delta\psi_i = -k_i^2\psi_i \quad \text{in } \Omega, \qquad (1)$$

$$\partial\psi_i/\partial n = 0 \quad \text{on } \partial\Omega, \qquad (2)$$

where $\partial\Omega$ denotes the boundary of $\Omega$, $\partial/\partial n$ is the outward normal derivative and $0 < k_1^2 \leq k_2^2 \leq \cdots$. More specifically, the efficiency factor $\gamma = \gamma(\Omega)$ is defined as

$$\gamma = \frac{k_2}{2\pi}\left(1 - \frac{k_1^2}{k_2^2}\right)^{1/4}\left[\frac{\int_\Omega |\nabla\psi_1|^2}{\max_\Omega |\nabla\psi_1|^2}\right]^{1/2} \qquad (3)$$

Since analytical expressions for $k_1$, $k_2$ and $\psi_1$ are not known for general domains, we restrict our attention to four families of shapes (rectangular, elliptical, parabolic, and rhombic) which can be parametrized by a single variable, $r$. For each of these shapes, r is the ratio of the height to the width, which we refer to as the aspect ratio. For rectangular, elliptical and parabolic regions, exact values of $\gamma = \gamma(r)$ were found by using respectively, trigonometric functions, Mathieu functions and parabolic cylinder functions. For rhombic regions, approximate efficiency factors were determined by using highly accurate collocation methods as described by Overfelt and Kenney (1990).

There are several notable features which can be drawn from this study. First, for the four types of regions considered here, the efficiency factor is maximized when the second and third eigenvalues